Bioorganic & Medicinal Chemistry xxx (2017) xxx–xxx

Contents lists available at ScienceDirect

Bioorganic & Medicinal Chemistry

journal homepage: www.elsevier.com/locate/bmc

Structure-activity relationship studies of G9a-like protein (GLP) inhibitors

Yan Xiong [a,b], Fengling Li [c], Nicolas Babault [a,b], Hong Wu [c], Aiping Dong [c], Hong Zeng [c], Xin Chen [a,b], Cheryl H. Arrowsmith [c,e], Peter J. Brown [c], Jing Liu [a,b], Masoud Vedadi [c,d,*], Jian Jin [a,b,*]

[a] Department of Pharmacological Sciences, Icahn School of Medicine at Mount Sinai, New York, NY 10029, United States
[b] Department of Oncological Sciences, Icahn School of Medicine at Mount Sinai, New York, NY 10029, United States
[c] Structural Genomics Consortium, University of Toronto, Toronto, Ontario M5G 1L7, Canada
[d] Department of Pharmacology and Toxicology, University of Toronto, Toronto, Ontario M5S 1A8, Canada
[e] Princess Margaret Cancer Centre and Department of Medical Biophysics, University of Toronto, Toronto, Ontario M5G 2M9, Canada

ARTICLE INFO

Article history:
Received 12 May 2017
Revised 10 June 2017
Accepted 13 June 2017
Available online xxxx

Keywords:
GLP
G9a
Inhibitor
Quinazoline
Quinoline

ABSTRACT

Given the high homology between the protein lysine methyltransferases G9a-like protein (GLP) and G9a, it has been challenging to develop potent and selective inhibitors for either enzyme. Recently, we reported two quinazoline compounds, MS0124 and MS012, as GLP selective inhibitors. To further investigate the structure–activity relationships (SAR) of the quinazoline scaffold, we designed and synthesized a range of analogs bearing different 2-amino substitutions and evaluated their inhibition potencies against both GLP and G9a. These studies led to the identification of two new GLP selective inhibitors, **13** (MS3748) and **17** (MS3745), with 59- and 65-fold higher potency for GLP over G9a, which were confirmed by isothermal titration calorimetry (ITC). Crystal structures of GLP and G9a in complex with **13** and **17** provide insight into the interactions of the inhibitors with both proteins. In addition, we generated GLP selective inhibitors bearing a quinoline core instead of the quinazoline core.

1. Introduction

GLP (euchromatic histone-lysine *N*-methyltransferase 1 (EHMT1) or lysine methyltransferase 1D (KMT1D)) and G9a (EHMT2 or KMT1C) are highly homologous protein lysine methyltransferases (PKMTs), sharing about 80% sequence identity in their SET (suppressor of variegation 3–9, enhancer of zeste and trithorax) domains.[1,2] GLP and G9a catalyze the transfer of the methyl group from the cofactor *S*-5′-adenosyl-L-methionine (SAM) to the ε-amino group of the targeted lysine residue in a variety of histone and nonhistone substrates, such as H3K9,[3,4] H1,[5,6] H3K27,[7–9] H3K56,[10] p53,[11] SIRT1,[12] reptin,[13] MyoD,[14] CDYL1,[15] WIZ,[15] and G9a.[16] Dysregulation of GLP and G9a has been associated with numerous human diseases, including cancer, inflammatory diseases, and neurodegenerative disorder.[17–24]

Earlier studies suggested that GLP and G9a form a catalytically active heterodimeric complex to catalyze H3K9 mono- and dimethylation.[3,4] Most of the subsequent studies have been focused on the function of G9a with the assumption that GLP would behave similarly.[25] More recent research challenged the above assumption and revealed GLP and G9a possess distinct physiological functions.[26] For example, whereas the ankyrin repeat domain of G9a preferentially binds to H3K9me2, the ankyrin repeat domain of GLP binds tightly to H3K9me1.[27] Disruption of the binding of GLP and G9a to methylated H3K9 by ankyrin repeat domain mutations resulted in drastic phenotypic difference in mice.[28] In addition, tissue-specific expression profiles are different for GLP and G9a. While G9a shows higher expression level in white adipose tissue (WAT) than in brown adipose tissue (BAT), GLP is highly enriched in BAT and is essential for brown cell fate and thermogenesis.[29] Moreover, GLP and G9a regulate distinct sets of genes and have different effects on proliferating myoblasts and on skeletal muscle terminal differentiation.[25]

Over the last decade, a number of quinazoline-containing compounds have been developed to selectively inhibit the methyltransferase activity of GLP and G9a.[1,2,30–42] High throughput screening led to the discovery of BIX01294 (**1**), which is the first potent and selective dual inhibitor of GLP and G9a.[1] Our group and others utilized structure-based design strategy in combination with SAR exploration and developed more potent compounds, such

* Corresponding authors at: Structural Genomics Consortium, University of Toronto, Toronto, Ontario M5G 1L7, Canada (M. Vedadi). Department of Pharmacological Sciences, Icahn School of Medicine at Mount Sinai, New York, NY 10029, United States (J. Jin).

E-mail addresses: m.vedadi@utoronto.ca (M. Vedadi), jian.jin@mssm.edu (J. Jin).

http://dx.doi.org/10.1016/j.bmc.2017.06.021
0968-0896/

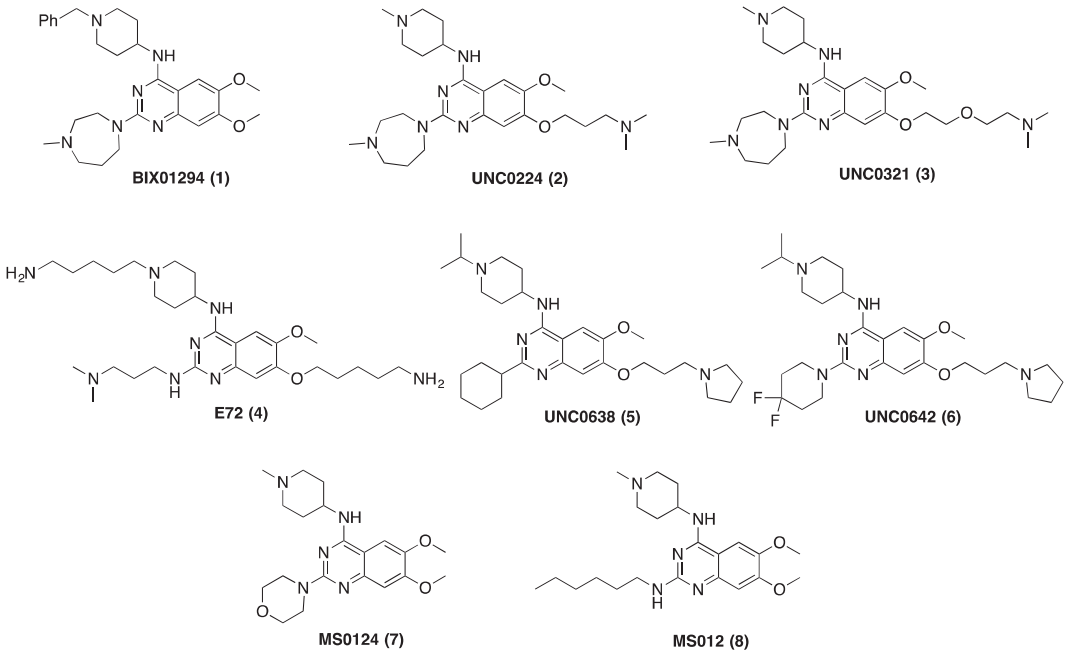

Fig. 1. Structures of selected G9a/GLP inhibitors.

as UNC0224 (**2**),[37] UNC0321 (**3**),[38] and E72 (**4**).[30] Optimization of physicochemical and pharmacokinetic properties of this scaffold led to a cellular chemical probe, UNC0638 (**5**),[35,40,43] and subsequently an *in vivo* chemical probe, UNC0642 (**6**).[36] Compounds **5** and **6** have been widely used as tool compounds by the research community to investigate the biological function and to test the therapeutic hypotheses associated with GLP and G9a.[43–45] Due to the fact that these compounds are dual inhibitors of GLP and G9a, the phenotypic effects rendered by these compounds could be attributed to the inhibition of methyltransferase activity of GLP and/or G9a. Hence, GLP or G9a selective inhibitors, which selectively inhibit GLP over G9a or vice versa, are required to dissect the distinct biological function of each enzyme. Recently, we screened our quinazoline compound collection against GLP and G9a and discovered a potent and selective GLP inhibitor, MS0124 (**7**).[46] Preliminary SAR guided optimization led to an improved GLP selective inhibitor, MS012 (**8**).[46] Compounds **7** and **8** share most of the substituent groups on the quinazoline core, except the 2-amino moiety. However, this important 2-amino region of the quinazoline scaffold has not been extensively explored in our previous study. Here, we describe our continued optimization of this region, which resulted in the discovery of two new GLP selective compounds, **13** and **17**. In addition, we report two GLP selective inhibitors bearing a quinoline core instead of the quinazoline core.

2. Results and discussion

2.1. Design and synthesis of quinazoline and quinoline derivatives

Through our previous SAR studies, we found that structural modifications to the 2-amino region of the quinazoline scaffold, which is shared by MS0124 and MS012, could drastically increase selectivity for GLP.[46] X-ray crystal structures of GLP and G9a in the complex with MS0124 or MS012 revealed virtually identical inhibitor–protein interactions, and did not provide informative insight to guide the design of more selective inhibitors.[46] Therefore, it is necessary to extensively explore a variety of amino substituents to understand the SAR trend at this 2-amino region.

2-Amino substituted quinazoline analogs were readily prepared using the efficient two-step synthetic sequence we developed previously.[37] Briefly, 4-chloro displacement of commercially available 2,4-dichloro-6,7-dimethoxyquinazoline with 4-amino-1-methylpiperidine yielded the intermediate **9**. Substitution of the 2-chloro group of the intermediate **9** with various amines under microwave conditions provided the desired quinazoline analogs **11**–**37** (Scheme 1).

In cocrystal structures of MS0124 and MS012, while the N1 nitrogen atom of the quinazoline core forms important hydrogen bonds with GLP and G9a, the N2 nitrogen atom does not interact with either protein. We attempted to replace the N2 nitrogen atom of the quinazoline core with a carbon atom, which leads to a structurally distinct quinoline core. Although quinoline analogs were reported as equipotent GLP and G9a dual inhibitors,[42] GLP selective inhibitors with a quinoline core have not been reported. Thus, we prepared the quinoline analogs of MS0124 and MS012 for direct comparison.

The quinoline analogs were synthesized from the commercially available 2,4-dichloro-6,7-dimethoxyquinoline through two consecutive Buchwald-Hartwig cross coupling reactions under microwave conditions. The first coupling reaction occured at the 2-chloro position to provide the intermediate **10**, which was then coupled with 4-amino-1-methylpiperidine at the 4-chloro position at an elevated temperature to yield desired quinoline products **38** and **39** (Scheme 2).

2.2. Results in GLP and G9a biochemical assays

We evaluated the potency of the synthesized compounds in GLP and G9a biochemical assays, which are radioactivity-based scintillation proximity assays that measure the transfer of the methyl group from ^{3}H-SAM to the peptide substrates.[36] We summarize the biochemical assay data (IC_{50} values) in Tables 1–3.

First, we assessed the potency and selectivity of a number of tertiary 2-amino analogs bearing a fixed *N*-methyl group (**11**–**28**, Table 1). Besides the previously reported analogs with a relatively long linear side chain (e.g., butyl, pentyl, hexyl),[46] we evaluated analogs with a short alkyl chain, such as methyl (**11**), ethyl (**12**),

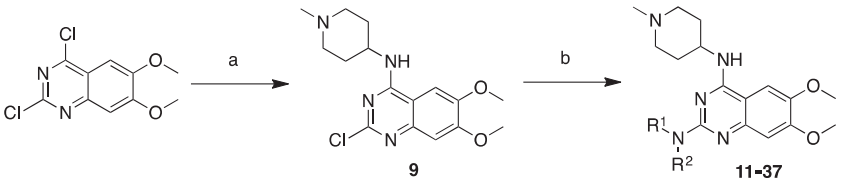

Scheme 1. Synthesis of 2-amino substituted quinazolines. Reagents and conditions: (a) 4-amino-1-methylpiperidine, K_2CO_3, DMF, rt, 90%; (b) R^1R^2NH, 4N HCl in dixoane, *i*PrOH, microwave, 160 °C, 75–85%.

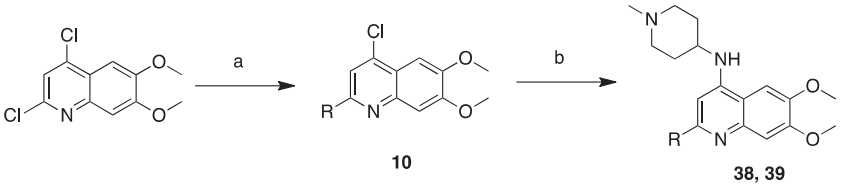

Scheme 2. Synthesis of quinoline analogs. Reagents and conditions: (a) amine, BINAP, $Pd_2(dba)_3$, *t*BuONa, THF, microwave, 100 °C, 45–50%; (b) 4-amino-1-methylpiperidine, BINAP, $Pd(OAc)_2$, *t*BuONa, THF, microwave, 160 °C, 70–71%.

Table 1
SAR of the tertiary amino substituted quinazolines.

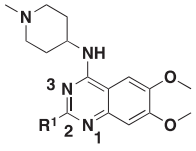

Compound	R^1	IC_{50} (nM)		Compound	R^1	IC_{50} (nM)	
		GLP	G9a			GLP	G9a
11		11 ± 3	191 ± 74	**22**		50 ± 18	726 ± 152
12		18 ± 5	465 ± 88	**23**	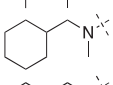	20 ± 3	532 ± 148
13 (MS3748)		5 ± 2	295 ± 103	**24**	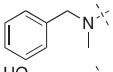	46 ± 9	534 ± 61
14		18 ± 2	318 ± 35	**25**	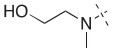	20 ± 2	282 ± 30
15		30 ± 8	550 ± 106	**26**	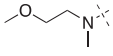	58 ± 17	1630 ± 230
16		17 ± 2	356 ± 90	**27**	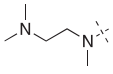	24 ± 6	151 ± 46
17 (MS3745)		4 ± 1	259 ± 80	**28**	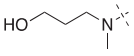	73 ± 25	484 ± 85
18		6 ± 2	177 ± 31	**29**		23 ± 6	343 ± 51
19	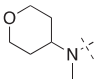	159 ± 5	1160 ± 510	**30**		20 ± 8	481 ± 129
20		43 ± 23	724 ± 209	**31**	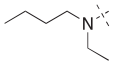	23 ± 4	508 ± 26
21		28 ± 4	359 ± 147	**32**	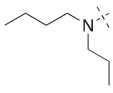	36 ± 15	443 ± 57

IC_{50} determination experiments were performed at substrate and cofactor concentrations equal to the respective K_m values for each enzyme. IC_{50} determination experiments were performed in triplicate and the values are presented as Mean ± SD.

Please cite this article in press as: Xiong Y., et al. Bioorg. Med. Chem. (2017), http://dx.doi.org/10.1016/j.bmc.2017.06.021

Table 2
SAR of the secondary amino substituted quinazolines.

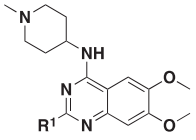

Compound	R^1	IC_{50} (nM)	
		GLP	G9a
33		77 ± 6	956 ± 362
34		24 ± 5	585 ± 145
35	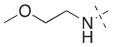	135 ± 27	1582 ± 526
36	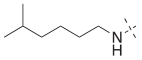	27 ± 13	315 ± 88
37	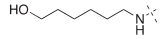	59 ± 18	788 ± 28

IC_{50} determination experiments were performed at substrate and cofactor concentrations equal to the respective K_m values for each enzyme. IC_{50} determination experiments were performed in triplicate and the values are presented as Mean ± SD.

Table 3
SAR of the quinoline scaffold.

Compound	Structure	IC_{50} (nM)	
		GLP	G9a
38	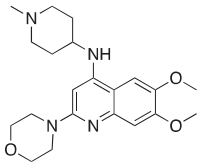	6 ± 2	92 ± 33
39	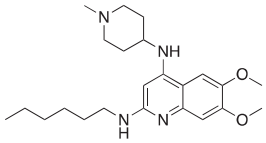	11 ± 4	110 ± 42

IC_{50} determination experiments were performed at substrate and cofactor concentrations equal to the respective K_m values for each enzyme. IC_{50} determination experiments were performed in triplicate and the values are presented as Mean ± SD.

and *n*-propyl (**13**) groups. Among these linear alkyl groups, the *n*-propyl group (**13**) resulted in the highest potency for GLP (IC_{50} = 5 ± 2 nM), with 59-fold selectivity for GLP over G9a (IC_{50} = 295 ± 103 nM). Switching the *n*-propyl group to *i*-propyl (**14**) decreased the potency for GLP by 4-fold (IC_{50} = 18 ± 2 nM) and decreased the selectivity for GLP over G9a to 18-fold. The cyclopropyl (**15**) group further decreased the potency for GLP (IC_{50} = 30 ± 8 nM). Enlarging the ring size from cyclopropyl (**15**) to cyclobutyl (**16**), cyclopentyl (**17**), and cyclohexyl (**18**) groups improved the potency for both GLP and G9a. Among these *N*-methyl-*N*-cycloalkyl substituted amino analogs, the cyclopentyl compound **17** displayed the best potency for GLP (IC_{50} = 4 ± 1 nM) and the best selectivity (65-fold) for GLP over G9a (IC_{50} = 259 ± 80 nM). Switching the cyclohexyl (**18**) group to the heteroatom containing tetrahydropyranyl (**19**) or aromatic phenyl (**20**) group greatly decreased the potency for both GLP and G9a and the selectivity for GLP over G9a. Since compound **13** is one of the most promising new GLP selective inhibitors, we synthesized and assessed more derivatives (**21**–**28**, Table 1) of this inhibitor. Branching the *n*-propyl group of **13** at the β-C position with a mono- (**21**) or di-methyl (**22**) group decreased the potency for GLP by 6- and 10-fold, respectively. Compared to the *n*-propyl group (**13**), cyclohexylmethyl (**23**) and benzyl (**24**) groups also led to weaker GLP inhibition. Similarly, heteroatom-containing groups, such as β-hydroxyethyl (**25**), β-methoxyethyl (**26**), β-dimethylaminoethyl (**27**) and γ-hydroxypropyl groups (**28**), did not improve either potency or selectivity in comparison with the *n*-propyl group of **13**. Next, we changed the fixed *N*-methyl group shared by compounds **11**–**28** to a fixed *N*-ethyl group in tertiary amino substituted compounds **29**–**31** (Table 1). These three *N*-ethyl bearing compounds showed similar potency for GLP and similar selectivity for GLP over G9a. Further increasing the length of this fixed group to a *N*-propyl (**32**) was also tolerated. However, none of these analogs carrying either *N*-ethyl or *N*-propyl group was more potent or more selective for GLP than their corresponding *N*-methyl analogs. Finally, we removed the fixed *N*-methyl group from compounds **18**, **22**, and **26** and prepared the corresponding secondary amino substituted analogs **33**, **34**, and **35** for direct comparison (Table 2). While compounds **34** and **35** showed comparable potency for GLP to that of **22** and **26**, compound **33** was a much weaker GLP inhibitor than **18** (23-fold decrease). In addition, a couple of analogs (**36** and **37**) of MS012 with a substituted *N*-hexyl group were also synthesized. However, both compounds were less potent than MS012 (GLP IC_{50} = 7 ± 2 nM; G9a IC_{50} = 992 ± 337 nM)[46] and were less selective for GLP over G9a than MS012. In summary, the SAR guided optimization on the 2-amino moiety of the quinazoline scaffold resulted in two new inhibitors, **13** and **17**, which have high potency (IC_{50} = ~5 nM) for GLP and high selectivity (~60-fold) for GLP over G9a.

The direct quinoline derivatives (compounds **38** and **39**) of MS0124 (GLP IC_{50} = 13 ± 4 nM; G9a IC_{50} = 440 ± 63 nM)[46] and MS012 were prepared and evaluated (Table 3). Both compounds retained high potency for GLP (**38**: IC_{50} = 6 ± 2 nM; **39**: IC_{50} = 11 ± 4 nM) and displayed improved potency for G9a (**38**: IC_{50} = 92 ± 33 nM; **39**: IC_{50} = 110 ± 42 nM). Whilst they were not as selective as the quinazoline analogs (MS0124 and MS012), compounds **38** and **39** favored the inhibition of GLP over G9a with 15-fold and 10-fold selectivity, respectively.

*2.3. Characterization of **13** and **17** in a biophysical assay*

The binding of **13** and **17** to GLP and G9a was assessed using isothermal titration calorimetry (ITC) in the presence of SAM (Fig. 2) as described previously.[46] Compound **13** displayed higher binding affinity to GLP (K_d = 57 ± 8 nM) than G9a (K_d = 510 ± 62 - nM). Similarly, compound **17** exhibited stronger binding affinity to GLP (K_d = 94 ± 14 nM) than G9a (K_d = 1070 ± 80 nM). Therefore, both compounds are confirmed to selectively bind to GLP over G9a in the ITC biophysical assay.

*2.4. Cocrystal structures of GLP and G9a in the complex with **13**, **17** and **18***

We solved the ternary structures of GLP and G9a in their complexes with compound **13**, **17**, or **18** in the presence of SAM (Fig. 3 and Supporting Fig. 1) with high resolution (1.4–1.85 Å). Consistent with the previously reported GLP selective inhibitors,[46] compounds **13, 17** and **18** adapt virtually identical inhibitor binding modes and ligand–protein interactions for both GLP and G9a (Fig. 3C, E, and Supporting Fig. 1C). Compounds **13, 17** and **18** occupy the substrate binding sites of GLP and G9a and form direct hydrogen bonds with two aspartic acids (D1176 and D1171 in GLP; D1088 and D1083 in G9a) and a water molecule. Superimposition

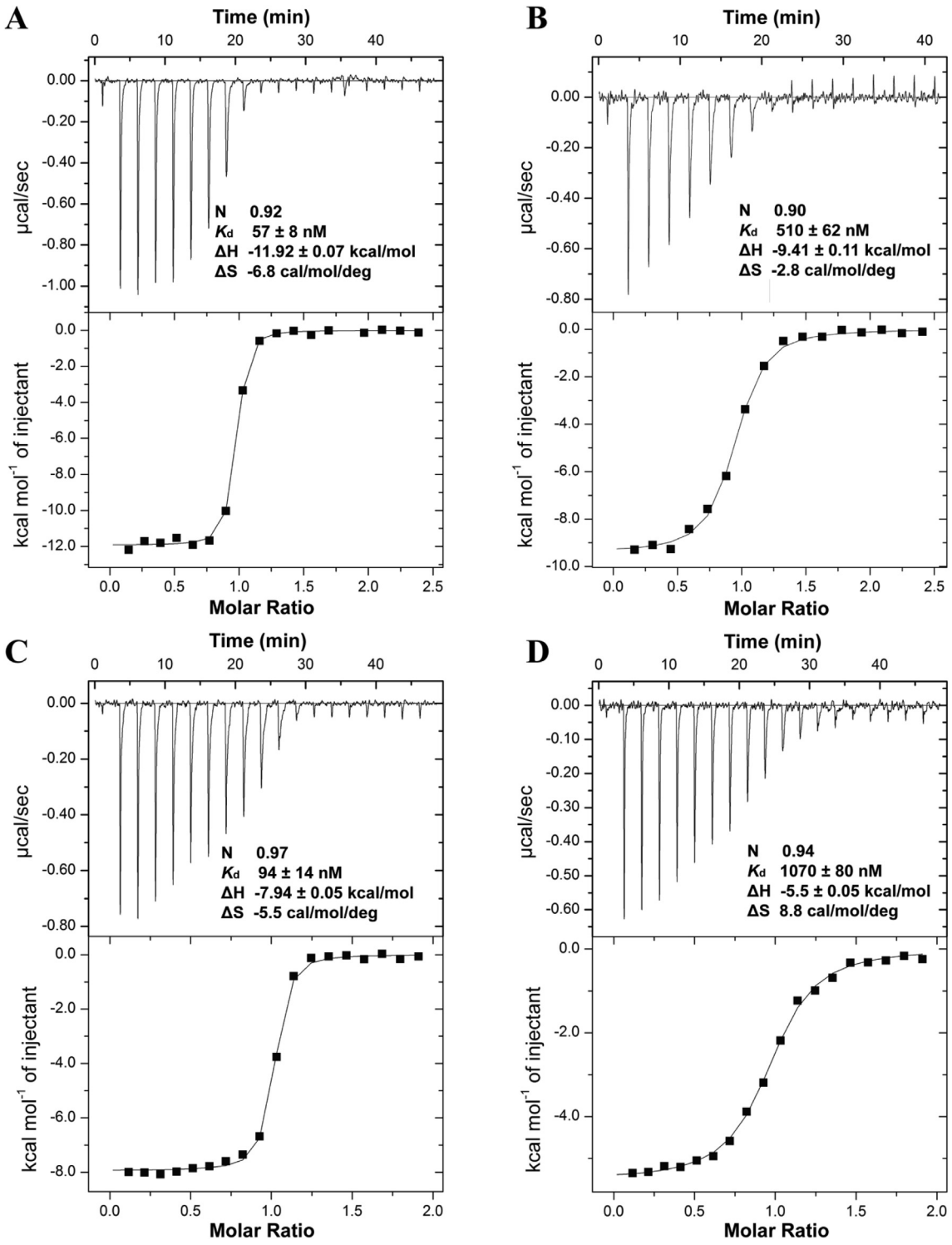

Fig. 2. Binding confirmation of **13** and **17**. Isothermal titration calorimetry (ITC) was used to confirm that **13** displayed better binding affinity to GLP (A) over G9a (B). Similarly, **17** also preferably bound to GLP (C) over G9a (D). ITC experiments were performed in triplicate.

of the GLP cocrystal structures of **13** and **17** with that of MS012,[46] MS0124,[46] and E72[30] reveals that the larger *N*-propyl group of **13** and *N*-cyclopentyl group of **17** point to the same direction as the *N*-hexyl group of MS012 and the smaller *N*-methyl groups of **13** and **17** direct to the site where the *N*-(3′-dimethylamino)propyl group of E72 is located (Fig. 3F). This is consistent with our previous hypothesis[46] that the *N*-(3′-dimethylamino)propyl group of E72 may adopt a sterically unfavorable geometry due to the strong charge-charge interaction between the dimethylamino group and GLP D1162.[30] Since these cocrystal structures could not provide conclusive explanation for the observed high selectivity, additional studies are being performed to understand the molecular basis for the high selectivity for GLP over G9a.

3. Conclusion

Extensive SAR studies around the 2-amino group of the quinazoline scaffold have led to the discovery of two new potent and

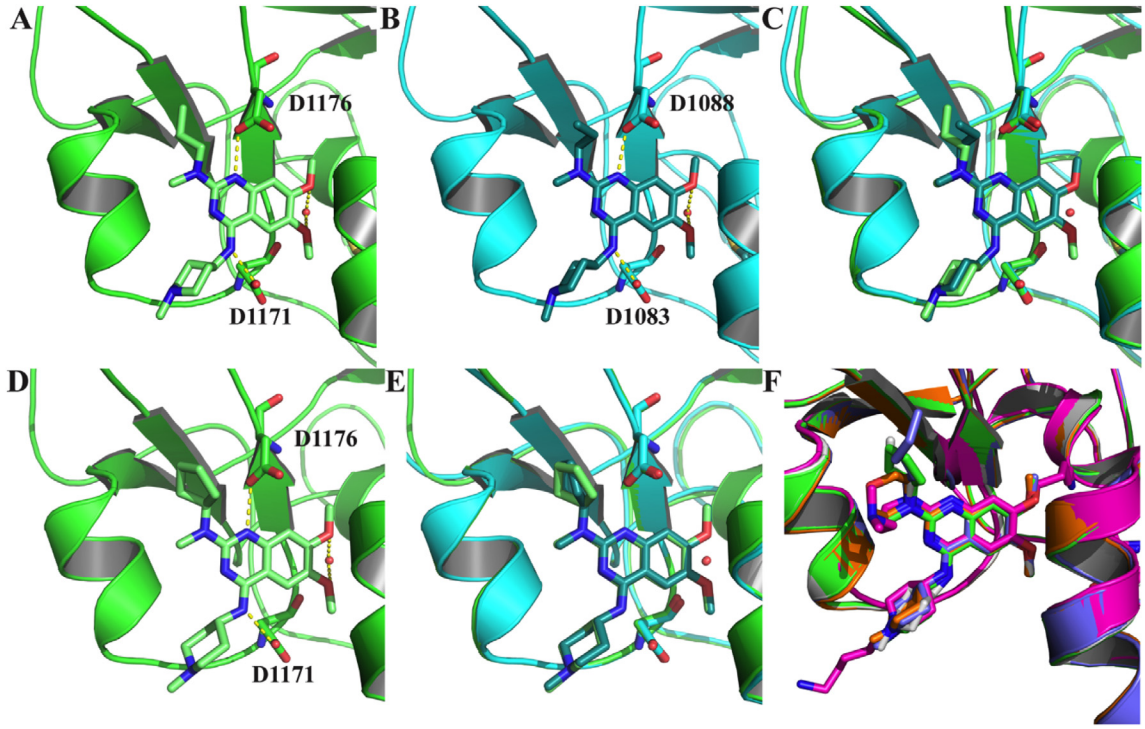

Fig. 3. X-ray cocrystal structures of GLP and G9a in complex with **13** and **17**. (A) Structure of GLP-SAM-**13** (green) (PDB code: 5VSD). (B) Structure of G9a-SAM-**13** (cyan) (PDB code: 5VSC). (C) Overlay of (A) and (B). (D) Structure of GLP-SAM-**17** (green) (PDB code: 5VSF). (E) Overlay of structures of (D) and G9a-SAM-**17** (cyan) (PDB code: 5VSE). (F) Overlay of GLP structures in the complex with **13** (gray), **17** (green), MS12 (blue), MS0124 (orange), and E72 (magenta). Water molecule is illustrated as a red sphere. Main interactions are shown in yellow dashed lines.

selective GLP inhibitors, **13** and **17**, both of which bear a tertiary acyclic amino group. The binding of **13** and **17** to GLP and G9a was confirmed by ITC. To determine inhibitor-protein interactions, we solved the cocrystal structures of GLP and G9a in their complexes with **13** and **17**. The structures revealed that the larger *N*-propyl group of **13** or *N*-cyclopentyl group of **17** occupies a sterically favorable binding site. In addition, we discovered two GLP selective inhibitors containing a quinoline core. Whilst these quinoline inhibitors are not as selective as their corresponding quinazoline analogs for GLP over G9a, the quinoline derivatives represent a chemically distinct scaffold that could be optimized in the future.

4. Experiment protocols

4.1. Chemistry

HPLC spectra for all compounds were acquired using an Agilent 1200 Series system with DAD detector. Chromatography was performed on a 2.1 × 150 mm Zorbax 300SB-C_{18} 5 μm column with water containing 0.1% formic acid as solvent A and acetonitrile containing 0.1% formic acid as solvent B at a flow rate of 0.4 mL/min. The gradient program was as follows: 1% B (0–1 min), 1–99% B (1–4 min), and 99% B (4–8 min). High-resolution mass spectra (HRMS) data were acquired in positive ion mode using an Agilent G1969A API-TOF with an electrospray ionization (ESI) source. Nuclear Magnetic Resonance (NMR) spectra were acquired on a Bruker DRX-600 spectrometer (600 MHz ^{1}H, 150 MHz ^{13}C) or a Varian Mercury spectrometer (400 MHz ^{1}H, 100 MHz ^{13}C). Chemical shifts are reported in ppm (δ). Preparative HPLC was performed on Agilent Prep 1200 series with UV detector set to 254 nm. Samples were injected into a Phenomenex Luna 75 × 30 mm, 5 μm, C_{18} column at room temperature. The flow rate was 40 mL/min. A linear gradient was used with 10% (or 50%) of MeOH (A) in H_2O (with 0.1 % TFA) (B) to 100% of MeOH (A). HPLC was used to establish the purity of target compounds. All final compounds had >95% purity using the HPLC methods described above.

4.1.1. 6,7-Dimethoxy-N^2,N^2-dimethyl-N^4-(1-methylpiperidin-4-yl) quinazoline-2,4-diamine (**11**)

Synthesis of the title compound was reported in this previous paper.[37]

4.1.2. N^2-Ethyl-6,7-dimethoxy-N^2-methyl-N^4-(1-methylpiperidin-4-yl)quinazoline-2,4-diamine (**12**)

The title compound (80% yield) was prepared according to synthetic procedures reported previously.[46] ^{1}H NMR (400 MHz, $CDCl_3$) δ 6.88 (s, 1H), 6.78 (s, 1H), 5.16 (d, J = 6.4 Hz 1H), 4.13–4.05 (m, 1H), 3.90 (s, 3H), 3.87 (s, 3H), 3.69 (q, J = 7.2 Hz, 2H), 3.15 (s, 3H), 2.85 (d, J = 12.0 Hz, 2H), 2.28(s, 3H), 2.16–2.11 (m, 4H), 1.64–1.56 (m, 2H), 1.15 (t, J = 6.8 Hz, 3H); MS (ESI) m/z 360.3 $[M+H]^+$.

4.1.3. 6,7-Dimethoxy-N^2-methyl-N^4-(1-methylpiperidin-4-yl)-N^2-propylquinazoline-2,4-diamine (**13**)

The title compound (82% yield) was prepared according to synthetic procedures for **12**. ^{1}H NMR (400 MHz, $CDCl_3$) δ 6.90 (s, 1H), 6.73 (s, 1H), 4.99 (d, J = 6.8 Hz 1H), 4.14–4.04 (m, 1H), 3.93 (s, 3H), 3.91 (s, 3H), 3.60 (t, J = 7.2 Hz, 2H), 3.19 (s, 3H), 2.88 (d, J = 12.0 Hz, 2H), 2.31 (s, 3H), 2.18–2.12 (m, 4H), 1.64–1.51 (m, 4H), 0.92 (t, J = 7.2 Hz, 3H); ^{13}C NMR (151 MHz, CD_3OD) δ 158.75, 158.61, 154.35, 147.97, 145.23, 103.90, 103.14, 102.73, 55.41, 54.77, 51.13, 44.85, 34.42, 30.94, 20.60, 10.38; HRMS (ESI-TOF) m/z: $[M+H]^+$ calcd for $C_{20}H_{32}N_5O_2$, 374.2551, found 374.2549.

*4.1.4. N^2-Isopropyl-6,7-dimethoxy-N^2-methyl-N^4-(1-methylpiperidin-4-yl)quinazoline-2,4-diamine (**14**)*

The title compound (76% yield) was prepared according to synthetic procedures for **12**. ^{1}H NMR (400 MHz, $CDCl_3$) δ 6.89 (s, 1H), 6.72 (s, 1H), 5.20–5.09 (m, 1H), 4.98 (d, J = 6.8 Hz 1H), 4.15–4.06 (m, 1H), 3.93 (s, 3H), 3.91 (s, 3H), 3.03 (s, 3H), 2.86 (d, J = 12.0 Hz, 2H), 2.32 (s, 3H), 2.20–2.15 (m, 4H), 1.66–1.57 (m, 2H), 1.18 (d, J = 6.8 Hz, 6H); MS (ESI) m/z 374.3 $[M+H]^+$.

*4.1.5. N^2-Cyclopropyl-6,7-dimethoxy-N^2-methyl-N^4-(1-methylpiperidin-4-yl)quinazoline-2,4-diamine (**15**)*

The title compound (79% yield) was prepared according to synthetic procedures for **12**. ^{1}H NMR (400 MHz, $CDCl_3$) δ 6.93 (s, 1H), 6.80 (s, 1H), 4.17 (d, J = 6.8 Hz, 1H), 4.19–4.11 (m, 1H), 3.90 (s, 3H), 3.87 (s, 3H), 3.17 (s, 3H), 2.86–2.83 (m, 2H), 2.87–2.69 (m, 1H), 2.28 (s, 3H), 2.17–2.09 (m, 4H), 1.63–1.53 (m, 2H), 0.82–0.78 (m, 2H), 0.67–0.65 (m, 2H); MS (ESI) m/z 372.3 $[M+H]^+$.

*4.1.6. N^2-Cyclobutyl-6,7-dimethoxy-N^2-methyl-N^4-(1-methylpiperidin-4-yl)quinazoline-2,4-diamine (**16**)*

The title compound (79% yield) was prepared according to synthetic procedures for **12**. ^{1}H NMR (400 MHz, $CDCl_3$) δ 6.90 (s, 1H), 6.75 (s, 1H), 5.21–5.12 (m, 1H), 5.06 (d, J = 7.2 Hz, 1H), 4.17–4.08 (m, 1H), 3.92 (s, 3H), 3.90 (s, 3H), 3.14 (s, 3H), 2.88–2.85 (m, 2H), 2.31 (s, 3H), 2.22–2.15 (m, 8H), 1.71–1.57 (m, 4H); MS (ESI) m/z 386.3 $[M+H]^+$.

*4.1.7. N^2-Cyclopentyl-6,7-dimethoxy-N^2-methyl-N^4-(1-methylpiperidin-4-yl)quinazoline-2,4-diamine (**17**)*

The title compound (76% yield) was prepared according to synthetic procedures for **12**. ^{1}H NMR (600 MHz, CD_3OD) δ 7.69 (s, 1H), 7.22 (s, 1H), 5.13–5.01 (br, 1H), 4.55 (tt, J = 12.3, 4.8 Hz, 1H), 4.00 (s, 3H), 3.96 (s, 3H), 3.69 (d, J = 12.8 Hz, 2H), 3.31–3.25 (m, 2H), 3.18 (s, 3H), 2.95 (s, 3H), 2.42 (d, J = 13.7 Hz, 2H), 2.09–1.98 (m, 4H), 1.91–1.84 (s, 2H), 1.82–1.72 (m, 4H); ^{13}C NMR (151 MHz, CD_3-OD) δ 158.45, 155.80, 152.87, 147.41, 103.54, 102.45, 99.12, 57.49, 55.58, 55.33, 54.02, 44.10, 29.84, 28.95, 28.24, 23.82. HRMS (ESI-TOF) m/z: $[M+H]^+$ calcd for $C_{22}H_{34}N_5O_2$, 400.2707, found 400.2705.

*4.1.8. N^2-Cyclohexyl-6,7-dimethoxy-N^2-methyl-N^4-(1-methylpiperidin-4-yl)quinazoline-2,4-diamine (**18**)*

The title compound (83% yield) was prepared according to synthetic procedures for **12**. ^{1}H NMR (400 MHz, $CDCl_3$) δ 6.89 (s, 1H), 6.68 (s, 1H), 4.90 (d, J = 6.8 Hz, 1H), 4.69–4.62 (m, 1H), 4.11–4.02 (m, 1H), 3.94 (s, 3H), 3.92 (s, 3H), 3.06 (s, 3H), 2.90–2.87 (m, 2H), 2.32 (s, 3H), 2.19–2.12 (m, 4H), 1.85–1.82 (m, 2H), 1.75–1.33 (m, 10*H*); MS (ESI) m/z 414.3 $[M+H]^+$.

*4.1.9. 6,7-Dimethoxy-N^2-methyl-N^4-(1-methylpiperidin-4-yl)-N^2-(tetrahydro-2H-pyran-4-yl)quinazoline-2,4-diamine (**19**)*

The title compound (80% yield) was prepared according to synthetic procedures for **12**. ^{1}H NMR (400 MHz, $CDCl_3$) δ 6.91 (s, 1H), 6.72 (s, 1H), 5.09–4.89 (m, 2H), 4.10–4.07 (m, 3H), 3.96 (s, 3H), 3.94 (s, 3H), 3.54 (t, J = 11.6 Hz, 2H), 3.09 (s, 3H), 2.91 (d, J = 12.0 Hz, 2H), 2.33 (s, 3H), 2.19–2.13 (m, 4H), 1.97–1.82 (m, 2H), 1.74–1.53 (m, 4H); MS (ESI) m/z 416.1 $[M+H]^+$.

*4.1.10. 6,7-Dimethoxy-N^2-methyl-N^4-(1-methylpiperidin-4-yl)-N^2-phenylquinazoline-2,4-diamine (**20**)*

The title compound (85% yield) was prepared according to synthetic procedures for **12**. ^{1}H NMR (400 MHz, $CDCl_3$) δ 7.37–7.31 (m, 4H), 7.16–7.13 (m, 1H), 6.96 (s, 1H), 6.75 (s, 1H), 5.02 (d, J = 6.8 Hz 1H), 3.94 (s, 3H), 3.91 (s, 3H), 3.77–3.68 (m, 1H), 3.60 (s, 3H), 2.77 (d, J = 12.0 Hz, 2H), 2.25 (s, 3H), 1.97 (d, J = 12.0 Hz, 2H), 1.90 (t, J = 12.0 Hz, 2H), 1.48 (qd, J = 12.0, 3.2 Hz, 2H); MS (ESI) m/z 408.1 $[M+H]^+$.

*4.1.11. N^2-Isobutyl-6,7-dimethoxy-N^2-methyl-N^4-(1-methylpiperidin-4-yl)quinazoline-2,4-diamine (**21**)*

The title compound (79% yield) was prepared according to synthetic procedures for **12**. ^{1}H NMR (400 MHz, $CDCl_3$) δ 6.90 (s, 1H), 6.75 (s, 1H), 5.05 (d, J = 6.8 Hz, 1H), 4.12–4.03 (m, 1H), 3.92 (s, 3H), 3.89 (s, 3H), 3.45 (d, J = 6.8 Hz, 2H), 3.19 (s, 3H), 2.87 (d, J = 12.4 Hz, 2H), 2.30 (s, 3H), 2.16–2.06 (m, 4H), 1.65–1.55 (m, 2H), 0.91 (d, J = 6.8 Hz, 6H); MS (ESI) m/z 388.3 $[M+H]^+$.

*4.1.12. 6,7-Dimethoxy-N^2-methyl-N^4-(1-methylpiperidin-4-yl)-N^2-neopentylquinazoline-2,4-diamine (**22**)*

The title compound (75% yield) was prepared according to synthetic procedures for **12**. ^{1}H NMR (400 MHz, $CDCl_3$) δ 6.92 (s, 1H), 6.71 (s, 1H), 4.94 (d, J = 6.4 Hz, 1H), 4.17–4.08 (m, 1H), 3.95 (s, 3H), 3.92 (s, 3H), 3.57 (s, 2H), 3.25 (s, 3H), 2.89 (d, J = 12.0 Hz, 2H), 2.32 (s, 3H), 2.17–2.12 (m, 4H), 1.67–1.57 (m, 2H), 0.98 (s, 9H); MS (ESI) m/z 402.3 $[M+H]^+$.

*4.1.13. N^2-(Cyclohexylmethyl)-6,7-dimethoxy-N^2-methyl-N^4-(1-methylpiperidin-4-yl)quinazoline-2,4-diamine (**23**)*

The title compound (81% yield) was prepared according to synthetic procedures for **12**. ^{1}H NMR (400 MHz, $CDCl_3$) δ 6.89 (s, 1H), 6.74 (s, 1H), 5.00 (d, J = 7.2 Hz, 1H), 4.14–4.03 (m, 1H), 3.93 (s, 3H), 3.90 (s, 3H), 3.47 (d, J = 7.2 Hz, 2H), 3.19 (s, 3H), 2.88 (d, J = 12.0 Hz, 2H), 2.31 (s, 3H), 2.17–2.10 (m, 4H), 1.83–1.76 (m, 1H), 1.73–1.70 (m, 4H), 1.65–1.56 (m, 3H), 1.21–1.13 (m, 3H), 1.00–0.91 (m, 2H); MS (ESI) m/z 428.2$[M+H]^+$.

*4.1.14. N^2-Benzyl-6,7-dimethoxy-N^2-methyl-N^4-(1-methylpiperidin-4-yl)quinazoline-2,4-diamine (**24**)*

The title compound (84% yield) was prepared according to synthetic procedures for **12**. ^{1}H NMR (400 MHz, $CDCl_3$) δ 7.29–7.24 (m, 4H), 7.23–7.17 (m, 1H), 6.93 (s, 1H), 6.79 (s, 1H), 5.13 (d, J = 6.8 Hz, 1H), 4.93 (s, 2H), 4.07–3.98 (m, 1H), 3.92 (s, 3H), 3.89 (s, 3H), 3.12 (s, 3H), 2.77 (d, J = 12.0 Hz, 2H), 2.26 (s, 3H), 2.03–2.01 (m, 4H), 1.58–1.49 (m, 2H); MS (ESI) m/z 422.3 $[M+H]^+$.

*4.1.15. 2-((6,7-Dimethoxy-4-((1-methylpiperidin-4-yl)amino) quinazolin-2-yl)(methyl)amino)ethan-1-ol (**25**)*

The title compound (78% yield) was prepared according to synthetic procedures for **12**. ^{1}H NMR (400 MHz, $CDCl_3$) δ 6.81 (s, 1H), 6.77 (s, 1H), 5.41 (d, J = 7.2 Hz, 1H), 4.13–4.03 (m, 1H), 3.88–3.87 (m, 2H), 3.87 (s, 3H), 3.85 (s, 3H), 3.74 (t, J = 4.8 Hz, 2H), 3.22 (s, 3H), 2.83 (d, J = 11.6 Hz, 2H), 2.27 (s, 3H), 2.16–2.09 (m, 4H), 1.67–1.57 (m, 2H); MS (ESI) m/z 376.2 $[M+H]^+$.

*4.1.16. 6,7-Dimethoxy-N^2-(2-methoxyethyl)-N^2-methyl-N^4-(1-methylpiperidin-4-yl)quinazoline-2,4-diamine (**26**)*

The title compound (75% yield) was prepared according to synthetic procedures for **12**. ^{1}H NMR (400 MHz, $CDCl_3$) δ 6.88 (s, 1H), 6.77 (s, 1H), 5.12 (d, J = 6.8 Hz, 1H), 4.12–4.03 (m, 1H), 3.90 (s, 3H), 3.88 (s, 3H), 3.82 (t, J = 4.8 Hz, 2H), 3.60 (t, J = 4.8 Hz, 2H), 3.35 (s, 3H), 3.23 (s, 3H), 2.84 (d, J = 11.6 Hz, 2H), 2.29 (s, 3H), 2.15–2.10 (m, 4H), 1.64–1.54 (m, 2H); MS (ESI) m/z 390.3 $[M+H]^+$.

*4.1.17. N^2-(2-(dimethylamino)ethyl)-6,7-dimethoxy-N^2-methyl-N^4-(1-methylpiperidin-4-yl)quinazoline-2,4-diamine (**27**)*

The title compound (80% yield) was prepared according to synthetic procedures for **12**. ^{1}H NMR (400 MHz, $CDCl_3$) δ 6.88 (s, 1H), 6.76 (s, 1H), 5.11 (d, J = 6.8 Hz, 1H), 4.16–4.09 (m, 1H), 3.91 (s, 3H), 3.89 (s, 3H), 3.77 (t, J = 7.2 Hz, 2H), 3.20 (s, 3H), 3.23 (s, 3H), 2.85 (d, J = 11.6 Hz, 2H), 2.52 (t, J = 8.0 Hz, 2H), 2.30 (s, 6H), 2.29 (s, 3H), 2.15–2.10 (m, 4H), 1.66–1.57 (m, 2H); MS (ESI) m/z 403.3 $[M+H]^+$.

Please cite this article in press as: Xiong Y., et al. Bioorg. Med. Chem. (2017), http://dx.doi.org/10.1016/j.bmc.2017.06.021

*4.1.18. 3-((6,7-Dimethoxy-4-((1-methylpiperidin-4-yl)amino) quinazolin-2-yl)(methyl)amino)propan-1-ol (**28**)*

The title compound (78% yield) was prepared according to synthetic procedures for **12**. ^{1}H NMR (600 MHz, CD_3OD) δ 7.69 (s, 1H), 7.17 (s, 1H), 4.67–4.58 (m, 1H), 3.98 (s, 3H), 3.94 (s, 3H), 3.94–3.85 (m, 2H), 3.72–3.66 (m, 4H), 3.33 (s, 3H), 3.26 (t, J = 12.0 Hz, 2H), 2.94 (s, 3H), 2.41–2.39 (m, 2H), 2.11–2.04 (m, 2H), 1.97–1.90 (m, 2H); MS (ESI) m/z 404.3 $[M+H]^+$.

*4.1.19. N^2,N^2-Diethyl-6,7-dimethoxy-N^4-(1-methylpiperidin-4-yl) quinazoline-2,4-diamine (**29**)*

Synthesis of the title compound was reported in this previous paper.[37]

*4.1.20. N^2-Ethyl-6,7-dimethoxy-N^4-(1-methylpiperidin-4-yl)-N^2-propylquinazoline-2,4-diamine (**30**)*

The title compound (79% yield) was prepared according to synthetic procedures for **12**. ^{1}H NMR (400 MHz, $CDCl_3$) δ 6.87 (s, 1H), 6.70 (s, 1H), 4.98–4.82 (m, 1H), 4.18–4.00 (m, 1H), 3.94 (s, 3H), 3.92 (s, 3H), 3.67 (q, J = 7.0 Hz, 2H), 3.59–3.48 (m, 2H), 2.88 (d, J = 11.8 Hz, 2H), 2.32 (s, 3H), 2.17–2.12 (m, 4H), 1.67–1.61(m, 4H), 1.20 (t, J = 7.0 Hz, 3H), 0.93 (t, J = 7.4 Hz, 3H); MS (ESI) m/z 388.3 $[M+H]^+$.

*4.1.21. N^2-Butyl-N^2-ethyl-6,7-dimethoxy-N^4-(1-methylpiperidin-4-yl) quinazoline-2,4-diamine (**31**)*

The title compound (80% yield) was prepared according to synthetic procedures for **12**. ^{1}H NMR (400 MHz, $CDCl_3$) δ 6.86 (s, 1H), 6.69 (s, 1H), 4.88 (d, J = 6.4 Hz, 1H), 4.15–4.06 (m, 1H), 3.95 (s, 3H), 3.93 (s, 3H), 3.67 (q, J = 6.8 Hz, 2H), 3.59 (t, J = 7.6 Hz, 2H), 2.88 (d, J = 12.0 Hz, 2H), 2.32 (s, 3H), 2.17–2.12 (m, 4H), 1.66–1.57 (m, 4H), 1.41–1.33 (m, 2H), 2.00 (t, J = 6.8 Hz, 3H); 0.96 (t, J = 7.2 Hz, 3H); MS (ESI) m/z 402.3 $[M+H]^+$.

*4.1.22. N^2-Butyl-6,7-dimethoxy-N^4-(1-methylpiperidin-4-yl)-N^2-propylquinazoline-2,4-diamine (**32**)*

The title compound (75% yield) was prepared according to synthetic procedures for **12**. ^{1}H NMR (400 MHz, $CDCl_3$) δ 6.85 (s, 1H), 6.71 (s, 1H), 4.92 (d, J = 6.8 Hz, 1H), 4.13–4.05 (m, 1H), 3.94 (s, 3H), 3.91 (s, 3H), 3.59–3.53 (m, 4H), 2.88 (d, J = 12.0 Hz, 2H), 2.31 (s, 3H), 2.17–2.12 (m, 4H), 1.66–1.57 (m, 6H), 1.41–1.35 (m, 2H), 2.00 (t, J = 6.8 Hz, 3H); 0.97–0.91 (m, 6H); MS (ESI) m/z 416.2 $[M+H]^+$.

*4.1.23. N^2-Cyclohexyl-6,7-dimethoxy-N^4-(1-methylpiperidin-4-yl) quinazoline-2,4-diamine (**33**)*

The title compound (77% yield) was prepared according to synthetic procedures for **12**.

^{1}H NMR (400 MHz, $CDCl_3$) δ 6.82 (s, 1H), 6.79 (s, 1H), 5.30 (br, 1H), 4.79 (br, 1H), 4.12–4.10 (m, 1H), 3.90 (s, 3H), 3.87 (s, 3H), 3.88–3.85 (m, 1H), 2.85 (d, J = 11.6 Hz, 2H), 2.29 (s, 3H), 2.14–2.04 (m, 6H), 1.73–1.70 (m, 2H), 1.61–1.59 (m, 3H), 1.39–1.33 (m, 2H), 1.25–1.19 (m, 3H); MS (ESI) m/z 400.3 $[M+H]^+$.

*4.1.24. 6,7-Dimethoxy-N^4-(1-methylpiperidin-4-yl)-N^2-neopentylquinazoline-2,4-diamine (**34**)*

The title compound (81% yield) was prepared according to synthetic procedures for **12**. ^{1}H NMR (400 MHz, $CDCl_3$) δ 6.84 (s, 1H), 6.77 (s, 1H), 5.18 (br, 1H), 4.53 (br, 1H), 4.15–4.13 (m, 1H), 3.91 (s, 3H), 3.88 (s, 3H), 3.29 (d, J = 6.4 Hz, 2H), 2.88–2.85 (m, 2H), 2.30 (s, 3H), 2.18–2.12 (m, 4H), 1.65–1.56 (m, 2H), 0.96 (s, 9H); MS (ESI) m/z 388.3 $[M+H]^+$.

*4.1.25. 6,7-Dimethoxy-N^2-(2-methoxyethyl)-N^4-(1-methylpiperidin-4-yl)quinazoline-2,4-diamine (**35**)*

The title compound (83% yield) was prepared according to synthetic procedures for **12**. ^{1}H NMR (400 MHz, $CDCl_3$) δ 6.85 (s, 1H), 6.81 (s, 1H), 5.30 (br, 1H), 4.12 (br, 1H), 4.15–4.10 (m, 1H), 3.90 (s, 3H), 3.87 (s, 3H), 3.62–3.58 (m, 2H), 3.57–3.53 (m, 2H), 3.36 (s, 3H), 2.85–2.82 (m, 2H), 2.28 (s, 3H), 2.15–2.10 (m, 4H), 1.60–1.57 (m, 2H); MS (ESI) m/z 376.2 $[M+H]^+$.

*4.1.26. 6,7-Dimethoxy-N^2-(5-methylhexyl)-N^4-(1-methylpiperidin-4-yl)quinazoline-2,4-diamine (**36**)*

The title compound (80% yield) was prepared according to synthetic procedures for **12**. ^{1}H NMR (600 MHz, CD_3OD) δ 7.43 (s, 1H), 6.81 (s, 1H), 4.23–4.18 (m, 1H), 3.91 (s, 3H), 3.90 (s, 3H), 3.40 (t, J = 7.2 Hz, 2H), 2.97 (d, J = 12.0 Hz, 2H), 2.33 (s, 3H), 2.19 (t, J = 12.0 Hz, 2H), 2.10 (d, J = 12.6 Hz, 2H), 1.74 (td, J = 12.0, 3.6 Hz, 2H), 1.64–1.53 (m, 3H), 1.45–1.37 (m, 2H), 1.30–1.24 (m, 2H), 0.91 (d, J = 7.8 Hz, 6H); MS (ESI) m/z 416.3 $[M+H]^+$.

*4.1.27. 6-((6,7-Dimethoxy-4-((1-methylpiperidin-4-yl)amino) quinazolin-2-yl)amino)hexan-1-ol (**37**)*

The title compound (75% yield) was prepared according to synthetic procedures for **12**. ^{1}H NMR (400 MHz, $CDCl_3$) δ 6.84 (s, 1H), 6.83 (s, 1H), 5.42 (d, J = 7.2 Hz 1H), 4.83 (br, 1H), 4.17–4.06 (m, 1H), 3.89(s, 3H), 3.86 (s, 3H), 3.59 (t, J = 6.4 Hz, 2H), 3.42–3.37 (m, 2H), 2.85–2.82 (m, 3H), 2.27(s, 3H), 2.12–2.08 (m, 4H), 1.62–1.50 (m, 6H), 1.42–1.22 (m, 4H); MS (ESI) m/z 418.1 $[M+H]^+$.

4.1.28. 4-(4-Chloro-6,7-dimethoxyquinolin-2-yl)morpholine

Morpholine (32 μL, 0.38 mmol), 2,4-dichloro-6,7-dimethoxyquinoline (102 mg, 0.39 mmol), $Pd_2(dba)_3$ (6 mg, 6.5 μmol), BINAP (6 mg, 9.6 μmol), and sodium *tert*-butoxide (63 mg, 0.65 mmol) were mixed·THF (2 mL) was added and the resulting suspension was heated at 100 °C. and stirred in the microwave for 20 min. The reaction mixture was filtered through filter paper with CH_2Cl_2 and concentrated. The residue was purified by HPLC to give the title compound (52 mg, 45% yield). ^{1}H NMR (400 MHz, $CDCl_3$) δ 7.24 (s, 1H), 7.09 (s, 1H), 6.89 (s, 1H), 3.98 (s, 3H), 3.97 (s, 3H), 3.87–3.77 (m, 4H), 3.64–3.54 (m, 4H).

*4.1.29. 6,7-Dimethoxy-N-(1-methylpiperidin-4-yl)-2-morpholinoquinolin-4-amine (**38**)*

4-(4-Chloro-6,7-dimethoxyquinolin-2-yl)morpholine (52 mg, 0.17 mmol), 1-methylpiperidin-4-amine (38 mg, 0.33 mmol), $Pd(OAc)_2$ (7 mg, 0.03 mmol), BINAP (35 mg, 0.06 mmol), and sodium *tert*-butoxide (25 mg, 0.26 mmol) were mixed·THF (2 mL) was added and the resulting suspension was heated at 120 °C. and stirred in the microwave for 20 min. The reaction mixture was filtered through filter paper with CH_2Cl_2 and concentrated. The residue was purified by HPLC to give the title compound (46 mg, 71% yield). ^{1}H NMR (400 MHz, $CDCl_3$) δ 7.07 (s, 1H), 6.74 (s, 1H), 5.87 (s, 1H), 4.35 (d, J = 7.2 Hz, 1H), 3.94 (s, 6H), 3.83 (t, J = 4.8 Hz, 4H), 3.56 (t, J = 4.8 Hz, 4H), 3.50–3.41 (m, 1H), 2.86–2.78 (m, 2H), 2.31 (s, 3H), 2.22–2.01 (m, 4H), 1.69–1.60 (m, 2H); MS (ESI) m/z 387.1 $[M+H]^+$.

*4.1.30. N^2-Hexyl-6,7-dimethoxy-N^4-(1-methylpiperidin-4-yl) quinoline-2,4-diamine (**39**)*

The title compound (35% over 2 steps) was prepared according to synthetic procedures for **38**. ^{1}H NMR (600 MHz, CD_3OD) δ 7.38 (s, 1H), 7.04 (s, 1H), 5.75 (s, 1H), 3.92 (s, 3H), 3.91 (s, 3H), 3.49–3.40 (m, 1H), 3.37–3.30 (m, 2H), 2.94 (d, J = 11.4 Hz, 2H), 2.32 (s, 3H), 2.19 (t, J = 11.5 Hz, 2H), 2.11 (d, J = 12.2 Hz, 2H), 1.77–1.68 (m, 2H), 1.67–1.62 (m, 2H), 1.50–1.40 (m, 2H), 1.39–1.32 (m, 4H), 0.93 (t, J = 6.7 Hz, 3H); MS (ESI) m/z 401.4 $[M+H]^+$.

Please cite this article in press as: Xiong Y., et al. Bioorg. Med. Chem. (2017), http://dx.doi.org/10.1016/j.bmc.2017.06.021

4.2. GLP and G9a IC_{50} determination[46]

Methyltransferase activity assays for G9a and GLP were performed by monitoring the incorporation of tritium-labeled methyl group to lysine 9 of H3 (1–25) peptide using Scintillation Proximity Assay (SPA). The enzymatic reactions were performed at 23 °C with 20 min incubation of 10 μl reaction mixture in 25 mM potassium phosphate pH 8.0, 1 mM EDTA, 2 mM $MgCl_2$, 0.01% Triton X-100 containing 8 μM of cold SAM and 2 μM of ^{3}H-SAM (Cat.# NET155-V250UC; Perkin Elmer; www.perkinelmer.com), 1 μM of biotinylated H3 (1–25), 5 nM G9a or GLP, and compound titrations from 1.5 nM to 25 μM. To stop the reactions, 10 μL of 7.5 M Guanidine hydrochloride was added, followed by 60 μl of buffer (20 mM Tris, pH 8.0), mixed and transferred to a 384-well Streptavidin coated Flash-plate (PerkinElmer, http://www.perkinelmer.ca). After mixing, the mixtures in Flash-plate were incubated for 2 h and the CPM counts were measured using Topcount plate reader (Perkin Elmer, www.perkinelmer.com). The CPM counts in the absence of compound for each dataset were defined as 100% activity. In the absence of the enzyme, the CPM counts in each data set were defined as background (0%). All enzymatic reactions were performed in triplicate and IC_{50} values were determined by fitting the data to Four Parameter Logistic equation using GraphPad Prism 7 software.

4.3. Isothermal titration calorimetry[46]

Isothermal titration calorimetry (ITC) measurements were made at 25 °C on a MicroCal ITC200 Instrument (Malvern Instruments). Co-concentrated G9a–SAM and GLP–SAM (protein/SAM molar ratio of 1:5) were diluted at 35 μM in ITC buffer [50 mM Tris (pH 8.0), 150 mM NaCl] supplemented with 1% DMSO. Compound **13** and **17** were prepared in DMSO at 50 mM and diluted to 0.5 mM in ITC buffer with a final DMSO concentration of 1%. Binding constants were calculated by fitting the data using the ITC data analysis module in Origin 7.0 (OriginLab Corp.).

4.4. Protein expression, purification, crystallization, data collection and structure determination for compounds ***13*** and ***17***

Human G9a and GLP catalytic domains were cloned, expressed and purified as previously described.[46] Purified G9a and GLP proteins at about 20 mg/ml were mixed with compound **13** and **17** at 1:4 molar ratio of protein:compound. The protein-compound complexes were crystallized using sitting drop vapor diffusion method at 20 °C by mixing equal volume of the protein solution with the reservoir solution containing 7% PEG 20 K, 1.4% v/v 1,4-dioxane, 10% glycerol, 0.07 M bicine, pH 9.0 (for GLP-**13**); 10% PEG 20 K, 1.4% v/v 1,4-dioxane, 10% glycerol, 0.1 M bicine, pH 9.0 (for GLP-**17**); 20% PEG3350, 10% glycerol, 0.2 M sodium bromide (for G9a-**13**); 20% PEG3350, 0.2 M sodium fluoride, 10% glycerol, 0.1 M Bis-Tris propane pH 6.5 (for G9a-**17**). All crystals were soaked in the corresponding mother liquor supplemented with 20% glycerol as cryoprotectant before flash freezing in liquid nitrogen.

X-ray diffraction data for the different complexes were all collected at 100 K at beamline 24ID-E of Advanced Photon Source (APS), Argonne National Laboratory. Data sets were processed using MOSFLM and SCALA from the CCP4 suite (1994). The structures of the G9a and GLP complexes were solved by molecular replacement using the PHASER[47] and the atomic model of the G9a and GLP SET domains (PDB code 5TUY and 5TUZ respectively). The locations of the bound molecules were determined from a Fo-Fc difference electron density map. REFMAC[48] and phenix.refine[49,50] were used for structure refinement. Graphic program COOT[51] was used for model building and visualization. Crystal diffraction data and refinement statistics for the structure are displayed in Supporting Tables 1 and 2.

Conflict of interest

Authors declare no financial/commercial conflicts of interest.

Acknowledgements

We thank Albina Bolotokova for compound management and Taraneh Hajian for protein purification. The research described here was supported by the grants R01GM103893, R01GM122749, and R01CA218600 (to J.J) from the U.S. National Institutes of Health. The SGC is a registered charity (number 1097737) that receives funds from AbbVie, Bayer Pharma AG, Boehringer Ingelheim, Canada Foundation for Innovation, Eshelman Institute for Innovation, Genome Canada, Innovative Medicines Initiative (EU/EFPIA) [ULTRA-DD grant no. 115766], Janssen, Merck & Co., Novartis Pharma AG, Ontario Ministry of Economic Development and Innovation, Pfizer, Fundação de Amparo à Pesquisa do Estado de São Paulo-FAPESP, Takeda, and the Wellcome Trust. We thank the staff at the 24-ID-E beamline of Advanced Photon Source (APS) at Argonne National Laboratory for facilitating X-ray data collection.

A. Supplementary data

Supplementary data associated with this article can be found, in the online version, at http://dx.doi.org/10.1016/j.bmc.2017.06.021.

References

1. Kubicek S, O'Sullivan RJ, August EM, et al. Reversal of H3K9me2 by a small-molecule inhibitor for the G9a histone methyltransferase. *Mol Cell*. 2007;25:473–481.
2. Chang Y, Zhang X, Horton JR, et al. Structural basis for G9a-like protein lysine methyltransferase inhibition by BIX-01294. *Nat Struct Mol Biol*. 2009;16:312–317.
3. Tachibana M, Sugimoto K, Nozaki M, et al. G9a histone methyltransferase plays a dominant role in euchromatic histone H3 lysine 9 methylation and is essential for early embryogenesis. *Genes Dev*. 2002;16:1779–1791.
4. Tachibana M, Ueda J, Fukuda M, et al. Histone methyltransferases G9a and GLP form heteromeric complexes and are both crucial for methylation of euchromatin at H3–K9. *Genes Dev*. 2005;19:815–826.
5. Trojer P, Zhang J, Yonezawa M, et al. Dynamic histone H1 isotype 4 methylation and demethylation by histone lysine methyltransferase G9a/KMT1C and the jumonji domain-containing JMJD2/KDM4 proteins. *J Biol Chem*. 2009;284:8395–8405.
6. Weiss T, Hergeth S, Zeissler U, et al. Histone H1 variant-specific lysine methylation by G9a/KMT1C and Glp1/KMT1D. *Epigenet Chromatin*. 2010;3:7.
7. Patnaik D, Chin HG, Esteve PO, Benner J, Jacobsen SE, Pradhan S. Substrate specificity and kinetic mechanism of mammalian G9a histone H3 methyltransferase. *J Biol Chem*. 2004;279:53248–53258.
8. Tachibana M, Sugimoto K, Fukushima T, Shinkai Y. SET domain-containing protein, G9a, is a novel lysine-preferring mammalian histone methyltransferase with hyperactivity and specific selectivity to lysines 9 and 27 of histone H3. *J Biol Chem*. 2001;276:25309–25317.
9. Wu H, Chen XZ, Xiong J, et al. Histone methyltransferase G9a contributes to H3K27 methylation in vivo. *Cell Res*. 2011;21:365–367.
10. Yu YX, Song CY, Zhang QY, et al. Histone H3 lysine 56 methylation regulates DNA replication through its interaction with PCNA. *Mol Cell*. 2012;46:7–17.
11. Huang J, Dorsey J, Chuikov S, et al. G9a and Glp methylate lysine 373 in the tumor suppressor p53. *J Biol Chem*. 2010;285. 18122-18122.
12. Moore KE, Carlson SM, Camp ND, et al. A general molecular affinity strategy for global detection and proteomic analysis of lysine methylation. *Mol Cell*. 2013;50:444–456.
13. Lee JS, Kim Y, Kim IS, et al. Negative regulation of hypoxic responses via induced reptin methylation. *Mol Cell*. 2010;39:71–85.
14. Ling BMT, Bharathy N, Chung TK, et al. Lysine methyltransferase G9a methylates the transcription factor MyoD and regulates skeletal muscle differentiation. *Proc Natl Acad Sci U S A*. 2012;109:841–846.
15. Rathert P, Dhayalan A, Murakami M, et al. Protein lysine methyltransferase G9a acts on non-histone targets. *Nat Chem Biol*. 2008;4:344–346.
16. Sampath SC, Marazzi I, Yap KL, et al. Methylation of a histone mimic within the histone methyltransferase G9a regulates protein complex assembly. *Mol Cell*. 2007;27:596–608.

17. Benevento M, van de Molengraft M, van Westen R, van Bokhoven H, Kasri NN. The role of chromatin repressive marks in cognition and disease: a focus on the repressive complex GLP/G9a. *Neurobiol Learn Mem*. 2015;124:88–96.
18. Kleefstra T, Smidt M, Banning MJG, et al. Disruption of the gene euchromatin histone methyl transferase1 (Eu-HMTase1) is associated with the 9q34 subtelomeric deletion syndrome. *J Med Genet*. 2005;42:299–306.
19. Mozzetta C, Pontis J, Ait-Si-Ali S. Functional crosstalk between lysine methyltransferases on histone substrates: the case of G9A/GLP and polycomb repressive complex 2. *Antioxid Redox Signaling*. 2015;22:1365–1381.
20. Schaefer A, Sampath SC, Intrator A, et al. Control of cognition and adaptive behavior by the GLP/G9a epigenetic suppressor complex. *Neuron*. 2009;64:678–691.
21. Watanabe H, Soejima K, Yasuda H, et al. Deregulation of histone lysine methyltransferases contributes to oncogenic transformation of human bronchoepithelial cells. *Cancer Cell Int*. 2008;8:15.
22. Kaniskan HU, Jin J. Chemical probes of histone lysine methyltransferases. *ACS Chem Biol*. 2015;10:40–50.
23. Kaniskan HU, Konze KD, Jin J. Selective inhibitors of protein methyltransferases. *J Med Chem*. 2015;58:1596–1629.
24. Kaniskan HU, Martini ML, Jin J. Inhibitors of protein methyltransferases and demethylases. *Chem Rev*. 2017. http://dx.doi.org/10.1021/acs.chemrev.6b00801.
25. Battisti V, Pontis J, Boyarchuk E, et al. Unexpected distinct roles of the related histone H3 lysine 9 methyltransferases G9a and G9a-like protein in myoblasts. *J Mol Biol*. 2016;428:2329–2343.
26. Kramer JM. Regulation of cell differentiation and function by the euchromatin histone methyltranserfases G9a and GLP. *Biochem Cell Biol*. 2016;94:26–32.
27. Collins RE, Northrop JP, Horton JR, et al. The ankyrin repeats of G9a and GLP histone methyltransferases are mono- and dimethyllysine binding modules. *Nat Struct Mol Biol*. 2008;15:245–250.
28. Liu N, Zhang ZQ, Wu H, et al. Recognition of H3K9 methylation by GLP is required for efficient establishment of H3K9 methylation, rapid target gene repression, and mouse viability. *Genes Dev*. 2015;29:379–393.
29. Ohno H, Shinoda K, Ohyama K, Sharp LZ, Kajimura S. EHMT1 controls brown adipose cell fate and thermogenesis through the PRDM16 complex. *Nature*. 2013;504:163–167.
30. Chang YQ, Ganesh T, Horton JR, et al. Adding a lysine mimic in the design of potent inhibitors of histone lysine methyltransferases. *J Mol Biol*. 2010;400:1–7.
31. Chen WL, Wang ZH, Feng TT, et al. Discovery, design and synthesis of 6H-anthra [1,9-cd]isoxazol-6-one scaffold as G9a inhibitor through a combination of shape-based virtual screening and structure-based molecular modification. *Bioorg Med Chem*. 2016;24:6102–6108.
32. Devkota K, Lohse B, Liu Q, et al. Analogues of the natural product sinefungin as inhibitors of EHMT1 and EHMT2. *ACS Med Chem Lett*. 2014;5:293–297.
33. Kondengaden SM, Luo LF, Huang K, et al. Discovery of novel small molecule inhibitors of lysine methyltransferase G9a and their mechanism in leukemia cell lines. *Eur J Med Chem*. 2016;122:382–393.
34. Konze KD, Pattenden SG, Liu F, et al. A chemical tool for in vitro and in vivo precipitation of lysine methyltransferase G9a. *ChemMedChem*. 2014;9:549–553.
35. Liu F, Barsyte-Lovejoy D, Allali-Hassani A, et al. Optimization of cellular activity of G9a inhibitors 7-aminoalkoxy-quinazolines. *J Med Chem*. 2011;54:6139–6150.
36. Liu F, Barsyte-Lovejoy D, Li FL, et al. Discovery of an in vivo chemical probe of the lysine methyltransferases G9a and GLP. *J Med Chem*. 2013;56:8931–8942.
37. Liu F, Chen X, Allali-Hassani A, et al. Discovery of a 2,4-diamino-7-aminoalkoxyquinazoline as a potent and selective inhibitor of histone lysine methyltransferase G9a. *J Med Chem*. 2009;52:7950–7953.
38. Liu F, Chen X, Allali-Hassani A, et al. Protein lysine methyltransferase G9a inhibitors: design, synthesis, and structure activity relationships of 2,4-diamino-7-aminoalkoxy-quinazolines. *J Med Chem*. 2010;53:5844–5857.
39. Sweis RF, Pliushchev M, Brown PJ, et al. Discovery and development of potent and selective inhibitors of histone methyltransferase G9a. *ACS Med Chem Lett*. 2014;5:205–209.
40. Vedadi M, Barsyte-Lovejoy D, Liu F, et al. A chemical probe selectively inhibits G9a and GLP methyltransferase activity in cells. *Nat Chem Biol*. 2011;7. 648-648.
41. Yuan Y, Wang Q, Paulk J, et al. A small-molecule probe of the histone methyltransferase G9a induces cellular senescence in pancreatic adenocarcinoma. *ACS Chem Biol*. 2012;7:1152–1157.
42. Srimongkolpithak N, Sundriyal S, Li FL, Vedadi M, Fuchter MJ. Identification of 2,4-diamino-6,7-dimethoxyquinoline derivatives as G9a inhibitors. *Medchemcomm*. 2014;5:1821–1828.
43. Lehnertz B, Pabst C, Su L, et al. The methyltransferase G9a regulates HoxA9-dependent transcription in AML. *Genes Dev*. 2014;28:317–327.
44. Kim Y, Lee HM, Xiong Y, et al. Targeting the histone methyltransferase G9a activates imprinted genes and improves survival of a mouse model of Prader-Willi syndrome. *Nat Med*. 2017;23:213–222.
45. Simon JM, Parker JS, Liu F, et al. A role for widely interspaced Zinc finger (WIZ) in retention of the G9a methyltransferase on chromatin. *J Biol Chem*. 2015;290:26088–26102.
46. Xiong Y, Li F, Babault N, et al. Discovery of potent and selective inhibitors for G9a-like protein (GLP) lysine methyltransferase. *J Med Chem*. 2017;60:1876–1891.
47. McCoy AJ, Grosse-Kunstleve RW, Adams PD, Winn MD, Storoni LC, Read RJ. Phaser crystallographic software. *J Appl Crystallogr*. 2007;40:658–674.
48. Murshudov GN, Vagin AA, Dodson EJ. Refinement of macromolecular structures by the maximum-likelihood method. *Acta Crystallogr D Biol Crystallogr*. 1997;53:240–255.
49. Adams PD, Afonine PV, Bunkoczi G, et al. PHENIX: a comprehensive Python-based system for macromolecular structure solution. *Acta Crystallogr D Biol Crystallogr*. 2010;66:213–221.
50. Afonine PV, Grosse-Kunstleve RW, Echols N, et al. Towards automated crystallographic structure refinement with phenix.refine. *Acta Crystallogr D Biol Crystallogr*. 2012;68:352–367.
51. Emsley P, Cowtan K. Coot: model-building tools for molecular graphics. *Acta Crystallogr D*. 2004;60:2126–2132.